LETTER

doi:10.1038/nature11395

Room-temperature ferroelectricity in supramolecular networks of charge-transfer complexes

Alok S. Tayi[1]*, Alexander K. Shveyd[2]*, Andrew C.-H. Sue[2,3], Jodi M. Szarko[2,4,5], Brian S. Rolczynski[2,4,5], Dennis Cao[2,6], T. Jackson Kennedy[7], Amy A. Sarjeant[2], Charlotte L. Stern[2], Walter F. Paxton[2], Wei Wu[8], Sanjeev K. Dey[2], Albert C. Fahrenbach[2,6], Jeffrey R. Guest[9], Hooman Mohseni[8], Lin X. Chen[2,4,5], Kang L. Wang[3], J. Fraser Stoddart[2,6] & Samuel I. Stupp[1,2,10,11]

Materials exhibiting a spontaneous electrical polarization[1,2] that can be switched easily between antiparallel orientations are of potential value for sensors, photonics and energy-efficient memories. In this context, organic ferroelectrics[3,4] are of particular interest because they promise to be lightweight, inexpensive and easily processed into devices. A recently identified family of organic ferroelectric structures is based on intermolecular charge transfer, where donor and acceptor molecules co-crystallize in an alternating fashion known as a mixed stack[5–8]: in the crystalline lattice, a collective transfer of electrons from donor to acceptor molecules results in the formation of dipoles that can be realigned by an external field as molecules switch partners in the mixed stack. Although mixed stacks have been investigated extensively, only three systems are known[9,10] to show ferroelectric switching, all below 71 kelvin. Here we describe supramolecular charge-transfer networks that undergo ferroelectric polarization switching with a ferroelectric Curie temperature above room temperature. These polar and switchable systems utilize a structural synergy between a hydrogen-bonded network and charge-transfer complexation of donor and acceptor molecules in a mixed stack. This supramolecular motif could help guide the development of other functional organic systems that can switch polarization under the influence of electric fields at ambient temperatures.

Ordered networks of electron donors and acceptors are good candidates for organic ferroelectrics because of the possible long-range orientation of their charge-transfer dipoles. The canonical electron donor–acceptor systems—the mixed-stack tetrathiafulvalene (TTF) with halogenated quinones (Q)[2,3,7,11–13], like TTF·chloranil (TTF·QCl_4) and TTF·bromanil (TTF·QBr_4)—have been investigated by X-ray crystallography[7,11], vibrational spectroscopy[5,7,11,12] and electrical measurements[2,3,9,10,14]. The TTF·QCl_4 complex undergoes a ferroelectric phase transition at the Curie temperature ($T_C = 81$ K), evidenced by a discontinuous jump in ionicity (ρ) and dimerization into donor (D)–acceptor (A) pairs ($D^0 A^0 D^0 A^0 \rightarrow D^{\delta+}A^{\delta-} D^{\delta+}A^{\delta-}$); this dimerization breaks the centre of symmetry of the lattice. Categorizing this phase transition as a ferroelectric transition was first suggested[13] in 1991, when an anomalous spike in the dielectric constant was observed at T_C for TTF·QCl_4. In TTF·QBr_4, which is already ionic ($\rho > 0.5$) at room temperature, the molecules in the crystal have been shown to dimerize, giving donor–acceptor pairs at 53 K as result of a spin-Peierls instability[10,14,15]. In the ferroelectric ground state of these mixed-stack systems, measurable reversible polarization under an electric field has only been shown[9,10] for TTF·QCl_4, TTF·$QBrCl_3$ and TTF·QBr_4.

We describe here charge-transfer pairs that are capable of assembling into ordered three-dimensional supramolecular networks. This series of charge-transfer crystals is based on complexes between a pyromellitic diimide-based acceptor (**1** in Fig. 1a) and donors (**2**, **3** and **4** and Fig. 1a) that are derivatives of naphthalene, pyrene and TTF, respectively. These charge-transfer pairs co-crystallize (see below) under ambient conditions and the resulting solid-state superstructures were characterized (Supplementary Table 1) by X-ray crystallography (Fig. 1b–d). In these networks, the assembly of the acceptor (**1**) and donor (**2**, **3**, **4**) components in the lattice are stabilized by four primary non-covalent bonding interactions: charge-transfer, hydrogen-bonding, π–π stacking and van der Waals forces. Diimide **1** was functionalized with diethylene glycol 'arms' that are capable of acting as both donors and acceptors in the formation of hydrogen bonds. Electron-rich compounds **2**, **3** and **4** can also interact through hydrogen-bonding because their shorter 'arms' are terminated by hydroxyl or amino groups. An extensive hydrogen-bonded network, composed of interstack and intrastack hydrogen bonds (Fig. 1b–d), is formed during the self-assembly process. We refer to this modular design as lock arm supramolecular ordering (LASO), an approach which enables complementary molecules to crystallize rapidly into functional networks from solution under ambient conditions (Fig. 2a–c). The overall motif for LASO structures requires a hierarchical organization based on non-covalent bonding interactions that bridge distances from ångströms to nanometres and are considerably stronger than van der Waals forces. Locally, the charge-transfer and π–π stacking interactions are directed along a single direction parallel to the mixed-stack axis, while the hydrogen bonds extend into three dimensions. This panoply of supramolecular interactions leads to a tightly packed network of mixed stacks locked over larger length scales by hydrogen bonds, π–π stacking and charge transfer.

To illustrate the connectivity of the hydrogen-bonded network in the interstitial regions between the stacks, Hirshfeld surface analysis[16,17] was used to measure the distribution of close contact interactions (Fig. 2). The Hirshfeld surface is a graphical tool that compares the atomically averaged electron density of a molecule to the electron density of the entire crystal, and partitions the lattice into molecular surfaces that map the spatial contacts. White regions represent molecular contacts at the van der Waals distance, while red and blue portions represent lengths shorter and longer than the van der Waals distance, respectively (Fig. 2). This type of analysis helps identify which interactions are the most dominant among neighbouring stacks. In Fig. 2, the bar graphs on the left show that [O···H] interactions responsible for hydrogen-bonding make up 37–41% of all interstack contacts while [H···H] interactions are 42–50% of such contacts, revealing the close-packed nature of the superstructure. The lengths shorter than the van der Waals distance are significant because they

[1]Department of Materials Science and Engineering, Northwestern University, Evanston, Illinois 60208, USA. [2]Department of Chemistry, Northwestern University, Evanston, Illinois 60208, USA. [3]Department of Electrical Engineering, University of California, Los Angeles, Los Angeles, California 90095, USA. [4]ANSER Center, Northwestern University, Evanston, Illinois 60208, USA. [5]Chemical Sciences and Engineering Division, Argonne National Laboratory, Argonne, Illinois 60439, USA. [6]Graduate School of EEWS, Korea Advanced Institute of Science and Technology, Daejeon, 305-701, South Korea. [7]Department of Physics, Northwestern University, Evanston, Illinois 60208 USA. [8]Department of Electrical Engineering, Northwestern University, Evanston, Illinois 60208, USA. [9]Center for Nanoscale Materials, Argonne National Laboratory, Argonne, Illinois 60439, USA. [10]Department of Medicine, Northwestern University, Chicago, Illinois 60611, USA. [11]Institute for BioNanotechnology in Medicine, Northwestern University, Chicago, Illinois 60611, USA.
*These authors contributed equally to this work.

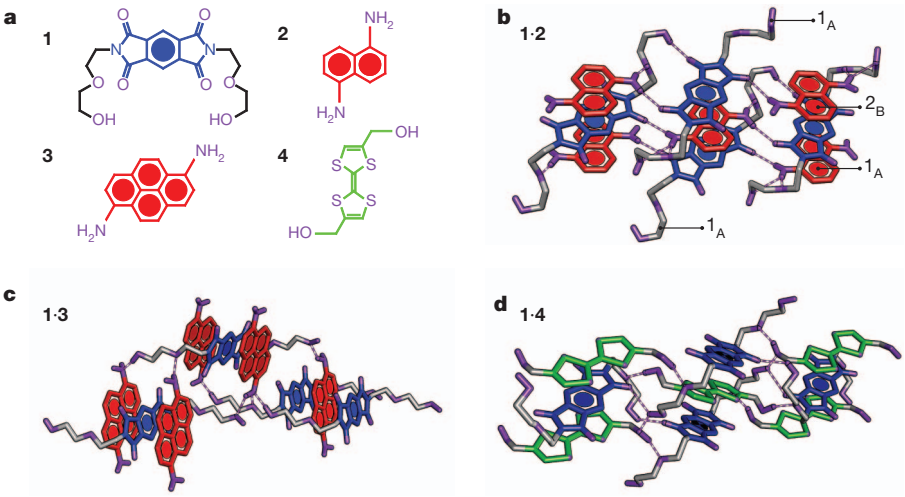

Figure 1 | Crystal structures of LASO complexes. **a**, Structural formulae of electron donor and acceptor molecules used in this research. Compound **1** is a pyromellitic diimide-based electron acceptor (blue). Compounds **2** and **3** are aromatic electron donors (red). Compound **4** is an electron-rich TTF derivative (green). The sites that participate in non-covalent bonding interactions are depicted in purple, and hydrogen bonds are depicted as purple dashed lines.

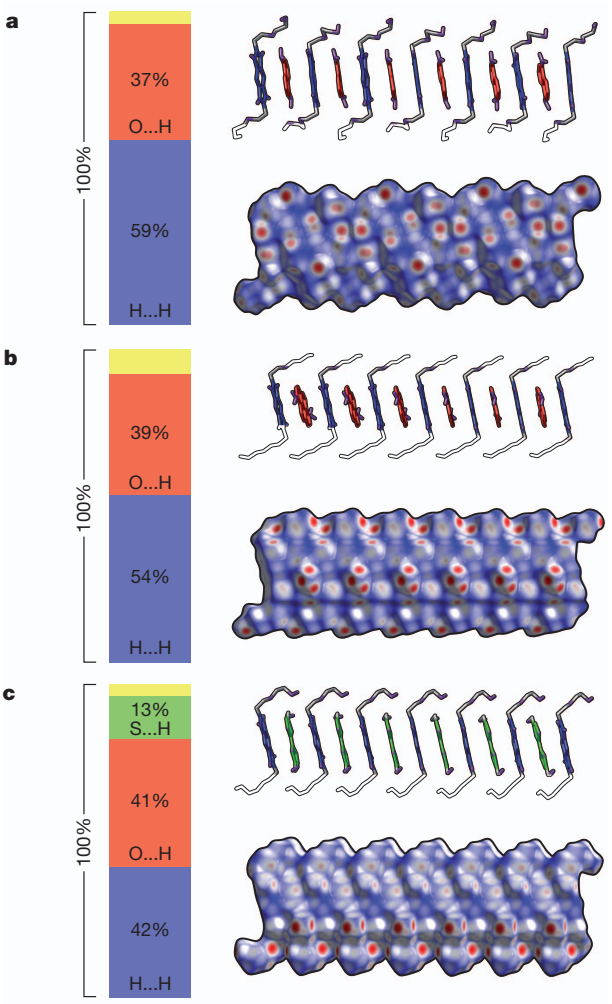

Figure 2 | Hirshfeld surface analysis. The Hirshfeld surface is a spatial map that uses colour coding to represent the proximity of close contacts around (a) molecule(s) within a network (white, distance (d) equals the van der Waals distance; blue, d exceeds the van der Waals distance; red, d is less than the van der Waals distance). Right, the Hirshfeld surface shown was calculated for $n = 13$ molecules within a stack for **1·2** (**a**), **1·3** (**b**) and **1·4** (**c**). In each panel **a**–**c**, the upper rectangle shows a portion of a donor–acceptor stack, while the lower region displays the corresponding Hirshfeld surface. Left, the percentage contribution of atomic contacts to the Hirshfeld surface is shown in the bar graph.

arise from short [O···H] and [H···H] distances when interstack hydrogen bonds are formed. These interstack interactions are between neighbouring arms and allow the stacks to pack tightly into a supramolecular network.

Because the electron transfer occurs along the stacking axis, we characterized ionicity[12,14], ρ, which is a measure of the extent of charge transfer, to investigate how its magnitude affects ferroelectric behaviour. Polarized vibrational spectroscopy[12,15] (Fourier transform infrared) was used to determine ρ for each complex (Supplementary Information). The *ungerade* modes were used to calculate[12] ρ because they are not influenced by electron–molecular vibrational interactions. At room temperature, ρ values for LASO complexes **1·2**, **1·3** and **1·4** (crystals shown in Fig. 3a–c) were determined by following the linear shift of the C=O stretch (1,728–1,716 cm^{-1}) polarized parallel to the donor–acceptor stack. Complexes **1·2** and **1·3** were found to be ionic with $\rho = 0.68$ and 0.89, respectively, while **1·4** lies close to the neutral–ionic border[12,13] ($\rho = 0.5$) with $\rho = 0.43$. The polar nature of the crystals enables, therefore, the LASO network to be ferroelectric. Along with significant electron transfer, a violation of the mutual exclusion rule

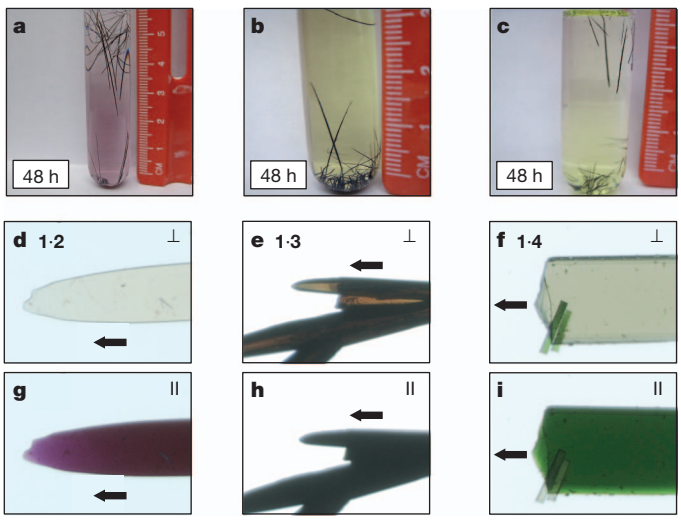

Figure 3 | Growth and charge-transfer anisotropy of LASO complexes. **a**–**c**, Images showing the growth of LASO networks **1·2** (**a**), **1·3** (**b**) and **1·4** (**c**) after 48 h. The long axis corresponds to the charge-transfer axis and the systems are single crystalline. **d**–**i**, Optical microscopy of very thin (<10 μm) co-crystals with linearly polarized white light. In **d**–**f**, light is polarized perpendicular to the long axis of the crystals for **1·2**, **1·3** and **1·4**, respectively. In **g**–**h**, the same structures are shown with the light polarized parallel to the charge-transfer axis, demonstrating the strong absorbance along a single axis on account of the photoexcitation of the donor–acceptor dimer.

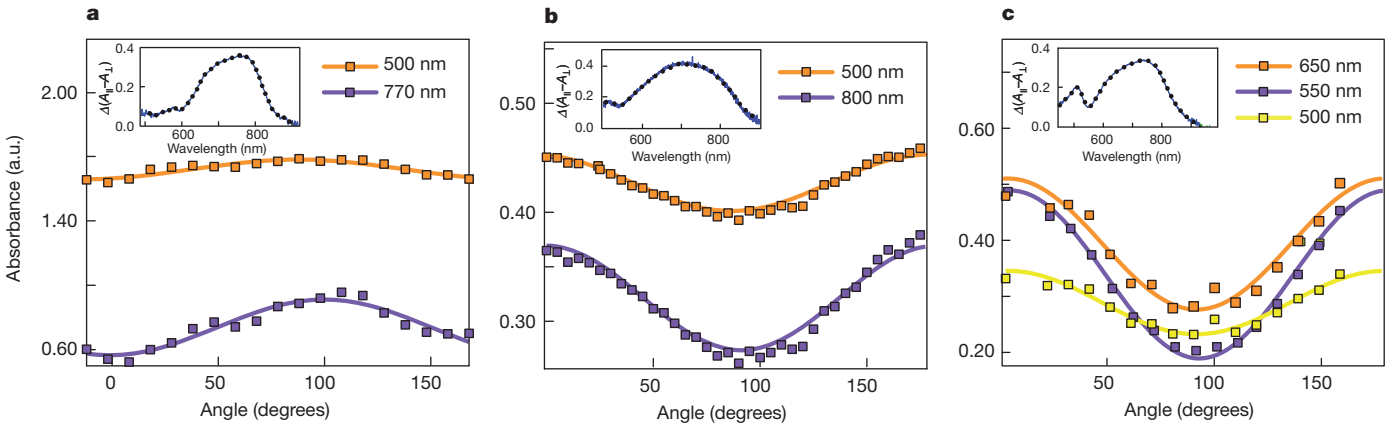

Figure 4 | Linear dichroism of LASO networks. a, **1·2**; **b**, **1·3**; **c**, **1·4**. When the electric field of linearly polarized light is oriented parallel to the charge-transfer axis, a strong absorbance is produced by the excitation of a donor–acceptor dimer ($D^{\delta+}A^{\delta-} \rightarrow [D^{\delta+}A^{\delta-}]^*$). The difference between the local minima (perpendicular polarizer orientation) and the local maxima (parallel polarizer orientation) of the absorbance will be largest at the onset of the charge-transfer band. The inset shows, as a function of wavelength, the difference in absorbance, $\Delta(A_{||} - A_{\perp})$, as a function of wavelength at parallel and perpendicular polarizations in transmission mode.

between the infrared and Raman modes[5,12,15] exists (Supplementary Information) in all three systems at 300 K, indicating a non-centrosymmetric lattice. This behaviour in mixed-stack crystals, composed of symmetric molecules, demonstrates that LASO networks fulfil the requirements for a ferroelectric system—namely donor–acceptor dimerization and a polar lattice.

Polarized optical microscopy (Fig. 3d–f) and polarized ultraviolet–visible transmission spectroscopy[18] (Fig. 4) were employed to elucidate the anisotropy of the charge-transfer in LASO networks with regard to the crystal axis. When the linear polarization of white light was oriented parallel to the polar mixed stack (long axis), the system absorbed intensely (Fig. 3g–i). Conversely, when the polarization was oriented perpendicular to the stack axis there was a clear lack of colour. The absorbance bands (Fig. 4a–c) associated with this colour change showed a maximum when the polarization was aligned with the direction of the stacks for **1·2**, **1·3** and **1·4** (Fig. 4a–c). These transitions (Fig. 4a–c, inset), located in the range 1.38–1.77 eV (700–900 nm), were attributed to the lowest intra-dimer charge-transfer exciton state[19] ($D^{\delta+}A^{\delta-} \rightarrow [D^{\delta+}A^{\delta-}]^*$). On the basis of this pronounced dichroism, it is possible to establish unequivocally that the polar axis of the material is aligned with the long axis of the crystal.

In order to determine the ferroelectric Curie temperature of each structure, the dielectric constant (ε_r) along the ferroelectric axis was measured[10] as a function of temperature. For crystals of **1·2**, **1·3** and **1·4**, no characteristic discontinuity was observed (Fig. 5a–c) between 5 K and 400 K. These results suggest that the ferroelectric phase exists at room temperature, an observation which is consistent with spectroscopic and crystallographic evidence. Further evidence for room-temperature ferroelectricity was obtained by measuring hysteresis curves of electric displacement versus electric field ($D-E$) along the ferroelectric axis (Fig. 6a, c and f). Polarization hysteresis was observed in complexes **1·2**, **1·3** and **1·4** at 300 K with remnant polarizations (P_r) exceeding 1 μC cm^{-2}. Attempts to observe saturation by applying higher electric fields resulted in dielectric breakdown and crystal melting. Larger polarization hysteresis loops were obtained at lower temperatures down to 7 K where leakage currents were minimized (Fig. 6b, d, e and g). At low temperature, $D-E$ curves for complex **1·4** were unexpectedly large. Surprisingly, the P_r for this network was found to be approximately 55 μC cm^{-2}, that is, much larger than for complexes **1·2** and **1·3**. This large polarization could result from the combination of the charge-transfer process and proton dynamics[3,4] within the crystal. The P_r of **1·4** at 7 K is amongst the highest reported[4,10,20,21] for organic ferroelectrics, and merits further study to elucidate the mechanism causing the polarization. However, the resistivity of all LASO systems investigated was found to be very high ($>10^9\,\Omega\,cm^{-1}$) at room temperature (Supplementary Information).

The ferroelectric curves obtained at room temperature were biased at a lower electric field than those obtained at cryogenic temperatures. At high electric fields at room temperature, dielectric leakage and Joule heating prevented the saturation of polarization hysteretic loops. Curves measured at 300 K were obtained by applying a smaller electric field than that required for saturation. As a result, these systems are inherently under-polarized and have smaller remnant polarizations than saturated loops. Even at these lower voltages, leakage

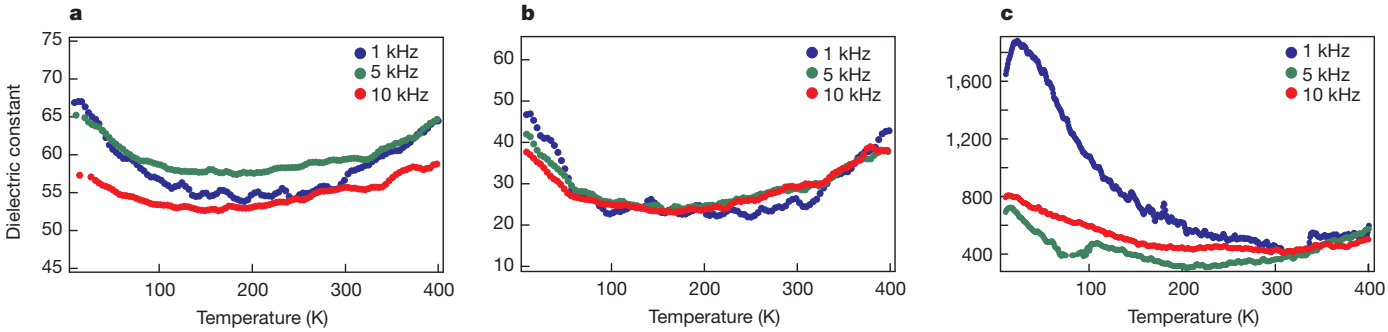

Figure 5 | Temperature-dependent dielectric constant measurements of LASO networks. The temperature-dependent dielectric constants were measured for complexes **1·2** (**a**), **1·3** (**b**) and **1·4** (**c**). Between 5 and 400 K, no reproducible characteristic discontinuity was observed in any of the networks. This observation indicates that the ferroelectric Curie temperatures, T_C, are likely to be outside the measurement range of the system. The dielectric constants for LASO networks were measured at 10 V with $f = 1$, 5 or 10 kHz.

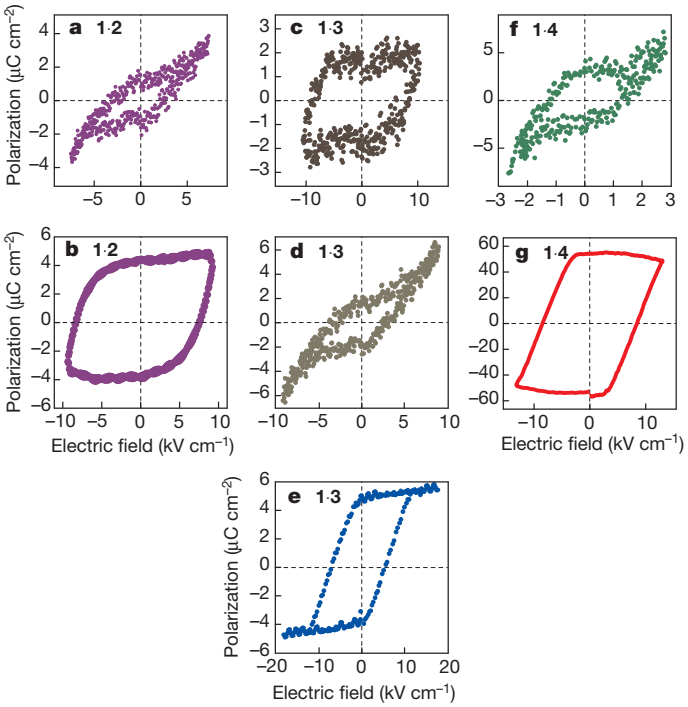

Figure 6 | Polarization hysteresis in supramolecular networks. Polarization versus electric field curves for LASO complexes **1·2** (**a**, **b**), **1·3** (**c**–**e**) and **1·4** (**f**, **g**). Polarization hysteresis curves for complex **1·2** were measured at 300 K (**a**) and 74 K (**b**), for complex **1·3** at 300 K (**c**, **d**) and 7 K (**e**), and for complex **1·4** at 300 K (**f**) and 7 K (**g**). Room-temperature hysteresis curves for LASO complexes are underpolarized because of leakage currents at high voltage. The ferroelectric network **1·3** showed hysteresis similar to that of **1·2** and **1·4** at small electric fields (**d**), and at higher electric fields revealed larger hysteresis loops (**c**). Hysteresis curve measurements were performed at $f = 0.1$ Hz (**a**–**e**, **g**) or $f = 1$ Hz (**f**).

current and degradation are possible, thus limiting the performance of devices.

Larger hysteresis loops were obtained (Fig. 6) in complex **1·3** at 300 K because this network is able to withstand higher voltages. It is interesting to note that this hydrogen-bonded network has the highest ionicity ($\rho \approx 0.89$) of all three materials presented here. The only charge-transfer ferroelectrics that demonstrate polarization bistability[9,10] are TTF·QCl_4, TTF·$QBrCl_3$ and TTF·QBr_4; for all three crystals, T_C occurs at cryogenic temperatures. As pointed out in ref. 22, high ionicities inhibit current flow in charge-transfer crystals because of Coulombic interactions. Negative and positive ions in a lattice can behave as ionic impurities that actively scatter moving electrons. Complexes that have large ionicities may therefore mitigate leakage current to some degree, for example, **1·3** and TTF·QBr_4. In this context, developing networks of charge-transfer complexes with large ionicities maybe a useful design rule to achieve ferroelectricity at room temperature and above.

Ferroelectric complexes **1·2** and **1·4**, when characterized by SQUID magnetometry, revealed magnetic hysteresis loops (Supplementary Information). Extensive elemental analysis described in Supplementary Information showed that any magnetic impurities present are below the present detection limits of inductively coupled plasma atomic emission spectroscopy. Other measurements described in Supplementary Information (magnetic force microscopy) were carried out in an attempt to verify the ferromagnetic behaviour. The small magnitude of the magnetization (Supplementary Fig. 14) in the hysteresis loop precludes us, however, from labelling these systems as ferromagnetic. Nonetheless, the unprecedented room-temperature ferroelectricity in these supramolecular networks and the observation of magnetization make the LASO design relevant to future explorations of multiferroic behaviour in metal-free systems at ambient temperatures.

In summary, we have developed a molecular design that allows donor and acceptor molecules to self-assemble into charge-transfer ferroelectric networks at ambient temperatures. The new structures challenge the long-standing notion that donor–acceptor mixed-stack materials cannot exhibit a ferroelectric T_C above room temperature. The demonstration of ferroelectric properties in an organic network affords us opportunities to produce these systems in new forms—such as electrically addressable hydrogels, ferroelectric catalysts and charge-transfer-based sensitizers for photovoltaics. The combination of donor–acceptor interactions with hydrogen-bonded networks offers a promising supramolecular platform to design novel organic electronic structures.

METHODS SUMMARY

Synthesis. Compound **1** was obtained (Supplementary Information) in one step by imidization[23] of the anhydride. The compound was purified by recrystallization from tetrahydrofuran and hexanes. Compounds **2** and **3** are commercially available, but were recrystallized from tetrahydrofuran and hexanes before use. The TTF-based donor **4** was synthesized using published procedures[24]. Standard purification was adequate to produce functional and robust ferroelectrics.

Network crystallization. The crystals were grown under darkness from a layered solvent system of 1-chlorobutane over 1,2-dichloroethane/diethyl ether (2/1 v/v %) at ambient temperatures. A dry 1:1 donor–acceptor mixture, with an acceptor (**1**) concentration of 2 mg ml^{-1} for **1·2**, 1 mg ml^{-1} for **1·3** and 0.5 mg ml^{-1} for **1·4**, produced crystals that grew to several centimetres in size in ~72 h after the first crystals had become visible (within 10 min). Anhydrous conditions are crucial for the growth of high-quality single crystalline networks. If traces of water are present in the solvent or the starting materials, growth is heavily branched (Supplementary Information) or sometimes even non-existent. Compound purity and concentration are also very important growth parameters. Impurities were found to induce epitaxial branching or even inhibit crystal growth, while concentration affects growth times and structure lengths.

Electronic measurements. The ferroelectric structures are mechanically robust and can be handled with vacuum tweezers. Gold wire electrodes (12.5 μm) were attached on either end using gold paint (Ted Pella Gold Paste). The resulting devices were tested for ferroelectricity in a physical properties measurement system (Quantum Design PPMS 6000) under an inert atmosphere. The temperature-dependent dielectric constants of LASO complexes were measured at 10 V with a 1, 5 or 10 kHz frequency. These measurements were performed using an Agilent E4980A LCR meter. Polarization hystereses were measured using a ferroelectric tester at 0.1 or 1 Hz frequency (Radiant Technologies Precision LC with Trek amplifier).

Received 4 June; accepted 11 July 2012.

1. Stupp, S. I. *et al.* Supramolecular materials: self-organized nanostructures. *Science* **276,** 384–389 (1997).
2. Horiuchi, S., Okimoto, Y., Kumai, R. & Tokura, Y. Quantum phase transition in organic charge-transfer complexes. *Science* **299,** 229–232 (2003).
3. Horiuchi, S. & Tokura, Y. Organic ferroelectrics. *Nature Mater.* **7,** 357–366 (2008).
4. Horiuchi, S. *et al.* Above-room-temperature ferroelectricity in a single-component molecular crystal. *Nature* **463,** 789–792 (2010).
5. Torrance, J. B., Vazquez, J. E., Mayerle, J. J. & Lee, V. Y. Discovery of a neutral-to-ionic phase-transition in organic materials. *Phys. Rev. Lett.* **46,** 253–257 (1981).
6. Tokura, Y. *et al.* Domain-wall dynamics in organic charge-transfer compounds with one-dimensional ferroelectricity. *Phys. Rev. Lett.* **63,** 2405–2408 (1989).
7. Collet, E. *et al.* Laser-induced ferroelectric structural order in an organic charge-transfer crystal. *Science* **300,** 612–615 (2003).
8. Hamilton, D. G., Lynch, D. E., Byriel, K. A. & Kennard, C. H. L. A neutral donor-acceptor π-stack: solid-state structures of 1:1 pyromellitic diimide-dialkoxynaphthalene cocrystals. *Aust. J. Chem.* **50,** 439–445 (1997).
9. Kobayashi, K. *et al.* Electronic ferroelectricity in a molecular crystal with large polarization directing antiparallel to ionic displacement. *Phys. Rev. Lett.* **108,** 237601 (2012).
10. Kagawa, F. *et al.* Electric-field control of solitons in a ferroelectric organic charge-transfer salt. *Phys. Rev. Lett.* **104,** 227602 (2010).
11. Torrance, J. B. *et al.* Anomalous nature of neutral-to-ionic phase-transition in tetrathiafulvalene-chloranil. *Phys. Rev. Lett.* **47,** 1747–1750 (1981).
12. Girlando, A., Marzola, F., Pecile, C. & Torrance, J. B. Vibrational spectroscopy of mixed stack organic semiconductors — neutral and ionic phases of tetrathiafulvalene chloranil (TTF-CA) charge-transfer complex. *J. Chem. Phys.* **79,** 1075–1085 (1983).
13. Okamoto, H. *et al.* Anomalous dielectric response in tetrathiafulvalene-*para*-chloranil as observed in temperature-induced and pressure-induced neutral-to-ionic phase-transition. *Phys. Rev. B* **43,** 8224–8232 (1991).
14. Soos, Z. G. Identification of dimerization phase transitions driven by Peierls and other mechanisms. *Chem. Phys. Lett.* **440,** 87–91 (2007).

15. Girlando, A., Pecile, C. & Torrance, J. B. A key to understanding ionic mixed stacked organic-solids — tetrathiafulvalene-bromanil (TTF-BA). *Solid State Commun.* **54,** 753–759 (1985).
16. McKinnon, J. J., Spackman, M. A. & Mitchell, A. S. Novel tools for visualizing and exploring intermolecular interactions in molecular crystals. *Acta Crystallogr. B* **60,** 627–668 (2004).
17. Crystal Explorer v.2.1 (Univ. Western Australia, Perth, 2007); available at http://hirshfeldsurface.net/.
18. Kuwata-Gonokami, M. *et al.* Exciton strings in an organic charge-transfer crystal. *Nature* **367,** 47–48 (1994).
19. Meneghetti, M. & Pecile, C. TTF-TCNE a charge transfer π-molecular crystal with partial ionic ground state: optical properties and electron-molecular vibrations interaction. *J. Chem. Phys.* **105,** 397–407 (1996).
20. Miyajima, D. *et al.* Ferroelectric columnar liquid crystal featuring confined polar groups within core–shell architecture. *Science* **336,** 209–213 (2012).
21. Zhang, Q. M., Bharti, V. & Zhao, X. Giant electrostriction and relaxor ferroelectric behavior in electron-irradiated poly(vinylidene fluoride-trifluoroethylene) copolymer. *Science* **280,** 2101–2104 (1998).
22. Torrance, J. B. The difference between metallic and insulating salts of tetracyanoquinodimethone (TCNQ): how to design an organic metal. *Acc. Chem. Res.* **12,** 79–86 (1979).
23. Brøndsted Nielsen, M., Hansen, J. G. & Becher, J. Self-complexing tetrathiafulvalene-based donor–acceptor macrocycles. *Eur. J. Org. Chem.* **1999,** 2807–2815 (1999).
24. Saha, S. *et al.* A photoactive molecular triad as a nanoscale power supply for a supramolecular machine. *Chem. Eur. J.* **11,** 6846–6858 (2005).

Supplementary Information is available in the online version of the paper.

Acknowledgements This work was supported by the Non-equilibrium Energy Research Center (NERC) at Northwestern University, funded by the US Department of Energy (DOE), Office of Basic Energy Sciences under award number DE-SC0000989. A.K.S. received support from the Materials Research Science and Engineering Centre (MRSEC) at Northwestern University, funded by the National Science Foundation (NSF). D.C., A.C.F. and J.F.S. were supported by the WCU program (R-31-2008-000-10055-0) at KAIST in Korea. Use of the Center for Nanoscale Materials was supported by the US Department of Energy, Office of Science, Office of Basic Energy Sciences, under contract no. DE-AC02-06CH11357. D.C. and A.C.F. were supported by NSF Graduate Research Fellowships. A.K.S. and A.C.-H.S. were supported by a fellowship from the NERC. A.S.T. was supported by a fellowship from the Initiative for Sustainability and Energy at Northwestern (ISEN) and NERC. We thank J. B. Ketterson and O. Chernyashevskyy (Northwestern University) for discussions and advice, Y. D. Shah (Northwestern University) for assistance with ferroelectricity measurements, A. M. Z. Slawin (University of St Andrews) for initial help with crystallographic data collection and refinement, M. Mara (Northwestern University) for assistance with spectroscopy, Y. Liu (The Molecular Foundry, Lawrence Berkeley National Laboratory) for discussions, and the Integrated Molecular Structure Education and Research Centre (IMSERC) and the Magnet and Low Temperature Facility at Northwestern University for providing access to equipment for the relevant experiments. Molecular crystal images were produced using the UCSF Chimera package from the Resource for Biocomputing, Visualisation and Informatics at the University of California, San Francisco.

Author Contributions A.S.T., A.K.S. and A.C.-H.S. conceived and designed the LASO networks. A.K.S., A.C.-H.S., D.C. and S.K.D. synthesized the compounds studied in this work; A.S.T., T.J.K. and W.W. performed device fabrication and testing; A.K.S., J.M.S. and B.R. performed spectroscopic studies. C.L.S. and A.A.S. collected crystallography data, and A.A.S. and A.K.S. performed crystal structure refinement; A.C.F. performed cyclic voltammetry experiments; J.R.G. helped with magnetic force microscopy experiments; H.M. provided testing equipment; J.F.S., S.I.S., L.X.C. and K.L.W. offered intellectual input; A.S.T., A.K.S., A.C.-H.S., J.F. S. and S.I.S. wrote the manuscript.

Author Information Reprints and permissions information is available at www.nature.com/reprints. The authors declare no competing financial interests. Readers are welcome to comment on the online version of the paper. Correspondence and requests for materials should be addressed to J.F.S. (stoddart@northwestern.edu) or S.I.S. (s-stupp@northwestern.edu).